

STUDY OF NEW MATERIALS FOR SOLAR CELLS

F. LAARIEDH ^{a*}, T. B. BADECHE ^a, A. LTAIEF ^{ab}, R. BOUSBIH ^a

^a*The Nanomaterials Laboratory, Department of Physics, University of Tabuk, Tabuk 71491, Kingdom of Saudi Arabia*

^b*Laboratory of Condensed Matter and Nanosciences, Molecular Electronic Components and Molecular Photovoltaics Team, Faculty of Sciences Monastir, Tunisia*

Today's thin film photovoltaic technologies are costly, toxic and rare in the earth's. Hence, in future cost reduction and increased production, using abundantly available non-toxic elements, seem to be the main issues like $\text{Cu}_2\text{ZnSnS}_4$ (CZTS), $\text{Cu}_2\text{ZnSnS}_4$ as an absorber layer material is attracting much attention recently in a heterojunction solar cell. $\text{ZnO}/\text{Cu}_2\text{ZnSnS}_4$ p-n heterostructure nanorod arrays were fabricated using ZnO nanorod arrays as the template was grown by the hydrothermal method and interpenetrated with CZTS and was studied by using Scanning Electron Microscopy (SEM) and High Resolution Transmission Electron Microscopy (HRTEM), which confirm the formation of CZTS nanocrystals (NCs). X-ray diffraction shows clearly the interpenetration of CZTS on ZnO nanorods. The results indicate that the heterostructure nanorod arrays may shed light on new opportunities for nanoscale solar cell.

(Received January 15, 2019; Accepted March 7, 2019)

Keywords: ZnO, CZTS, HRTEM, XRD, Solar cell

1. Introduction

The current global energy policy is orientated towards green-renewable and non-polluting energies, among which photovoltaics. The field of photovoltaics attracts the attention of scientists for many years at the fundamental level, and the technological progress made in recent years allows to consider, in the short and medium term, an economically advantageous industrial valorization. For the most part, the expected technological advances come from progress done in materials science, synthesis of new materials and in the manufacture of solar cells.

Among the most promising photovoltaic materials are semiconductors, some of which are already widely used in the field of optoelectronics. The leading material on which all semiconductor technology is currently based is silicon. However, some new complex materials (multi-atoms) compete with silicon because of their low cost and acceptable photovoltaic efficiency.

$\text{Cu}_2\text{ZnSnS}_4$ (CZTS), a p-type quaternary compound consists of abundant elements, is one of the promising candidate semiconductors for solar cell compounds because it has a high absorption coefficient of the order of 10^4 cm^{-1} with an optimum band gap of about 1.5 eV. [1–3] also, its toxicity is enough low compared to the compounds containing selenium and Cadmium telluride so that it is very attractive as a light absorber material for solar cells.[4–8]

The phase diagram of the Cu-Zn-Sn-Se system is rich in secondary phases. During the growth of the materials, these are in competition with the main phase $\text{Cu}_2\text{ZnSnSe}_4$ (CZTSe) targeted for its photovoltaic qualities. The secondary phases that may be present in the samples are, for example, ZnSe and Cu_2SnSe_3 (CTSe) [9-10]. Similarly, the secondary ZnS, Cu_2SnS_3 (CTS) phases can coexist in $\text{Cu}_2\text{ZnSnS}_4$ (CZTS) samples [11]. These secondary compounds will inevitably influence the properties electronic and optical CZTS and CZTSe, which may explain the great dispersion of measures [12]. Despite the sustained attention ternary compounds of the CTS

* Corresponding author : flaariedh@ut.edu.sa

and CZT type, their fundamental properties, such as crystalline structure and band gap, still on debate.

The CZTS quaternary compound thin layer was manufactured for the first time by Ito and Nakazawa 1988 using the spraying technique atomic beam in Shinshu University, these authors specified that the energy of the optical gap is close to the optimum value of 1.45eV. The phase transformation procedure on the quaternary structure of CZTSe had has been proposed by some groups of researchers [13]. Volobujeva et al. [14] made a thin layer of CZTSe by selenization of metal precursors of Sn-Zn-Cu in Se vapor contained in sealed ampoules of 250°C at 520°C. At low temperature, the dominant processes are the incorporation of Se and Cu outside the diffusion to form different selenium brass. This is due to Se, which reacts easily with Cu to form Cu_xSe_y at a lower temperature. As the temperature increases, the binary selenides and ternaries react with the excess of Se vapor and lead to the formation of $Cu_2ZnSnSe_4$.

Several research efforts have recently been made on the CZTS-based solar cells since Katagiri and al. reported a CZTS/CdS heterojunction solar cell with 6.77% [15–21].

2. Experimental details

ZnO nanorods were obtained using the hydrothermal technique. starting with the cleaning of conductive glass substrates (ITO, 10ohm/square) by ultrasound with acetone and isopropanol and acetic acid.

The substrates were coated at 2000 rpm for 20sec twice by centrifugation with a solution of 5 mM zinc acetate dehydrated in ethanol. To obtain small ZnO grains on the surface, the spin-coated substrates were placed in an oven at 350°C for 20 min. Then, the activated substrates were immersed in a solution of zinc nitrate and hexamethylenetetramine (HMT) with a 1: 1 ratio as precursors at a temperature of 90°C for 90 minutes to grow the ZnO nanorods in a system. isothermal sublimation with closed spacing. In order to obtain a well organized The substrate with the ZnO nanorods was placed in an oven around the quartz tube to maintain the system as a whole at an almost constant temperature of between 350 and 400°C.

Finally, a composite layer of (Cu,Sn)S was deposited on on the ZnO arrays by the successive ionic layer adsorption and reaction, SILAR method. In the SILAR approach, dissolved anionic and cationic precursors are in separate vessels. For one deposition cycle the bare nanostructured material is dipped into the precursor solution containing the metal cation. After rinsing, the nanostructured material is dipped into the second precursor solution containing the anion, and a second rinsing step completes the deposition cycle.

For the deposition, a mixed solution of Na_2S solutions was used as the anion precursor solution, and $SnCl_2$ and $CuCl_2$ were used as the cation precursor solution. After 40 cycles of SILAR processes, the composite CTS layer of (Cu,Sn)S was obtained with a concentration of Na_2S in the anion solution was 0.1M. And the concentration of Sn^{2+} and Cu^{2+} in the cation solution was 0.06M and 0.12M, respectively.

After the deposition of the CTS layer a thin film of (Cu, Zn)Sn CZT will be deposited. For the deposition of the ZnS film, $Zn(Ac)_2$, thiourea and sodium citrate solutions were prepared, respectively. Then were added into the $Zn(Ac)_2$ solution successively. Finally 3ml of ammonia was added to adjust the pH value of the deposition solution. The concentrations of the $Zn(Ac)_2$, thiourea and sodium citrate in the deposition solution were 0.04M, 0.12M, and 0.06M, respectively. After the preparation of deposition solution, glass substrates with the (Cu,Sn)S layer were inserted into the solution, and each substrate was placed at 60°C angle to the horizontal line. The depositions take place at 80°C for 3h.

This was followed by an annealing in a tubular furnace with quartz tube under a mixed N_2 and S vapor atmosphere with flow rate of N_2 1L/min at atmosphere pressure. The temperature of the precursor increased to 500°C in increments of 10°C/min. This temperature was kept constant for 2 hours then the system was allowed to cool naturally.

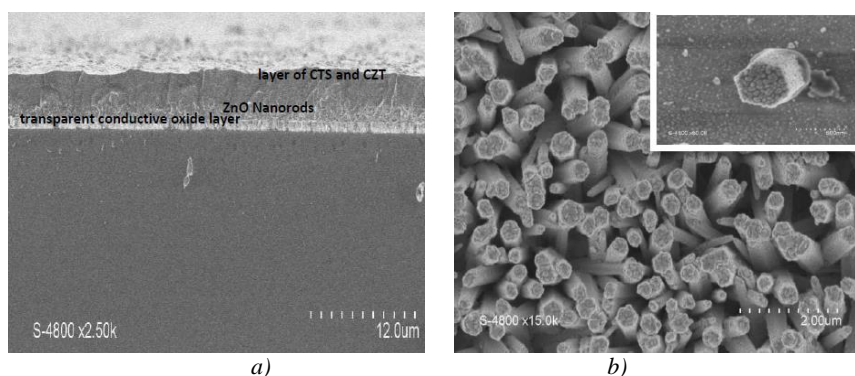


Fig. 1. (a) SEM Images of the ZnO as-grown film; (b) Scanning Electron Microscopy image of CTS-CZT / ZnO and high magnification SEM images of the CTS and CZT film.

The phase purity of the CZTS layer was assessed by X-ray diffraction (XRD) measurement, Raman spectra and scanning electron microscopy (SEM) and high resolution transmission electron microscopy (HRTEM) images, were measured in all the samples.

X-ray diffraction (XRD) patterns were taken in Bragg Brentano configuration using a Siemens D-5000 powder diffractometer with Cu K α radiation. The deconvolution for microstructural analysis was done with a B_6La certified sample. SEM images were obtained with a Hitachi S4800 electron microscope. HRTEM observations were performed using a JEOL JEM-2010 (High resolution mode: 0,16 nm point to point).

3. Discussion and results

Fig. 2 (a) is a typical SEM image shows the nanorods having a typical hexagonal morphology and satisfying vertical alignment. These NRs are nearly perpendicular to the substrate with lengths of about 2 μm and diameters around 200 nm. There are between 40 and 50 nanorods per square micron and the empty space between nanorods occupies around 40 - 45% of the whole surface.

In diffraction mode, the images of the high resolution electron microscopy show a single crystal diffraction pattern of ZnO nanorods (Fig 2-b) and showing a high crystalline quality contains one set of diffraction spots that can be indexed to the [010] zone axis of the ZnO, and other diffraction spots that can be easily indexed, within the same zone axis, as the (100) and (002) planes.

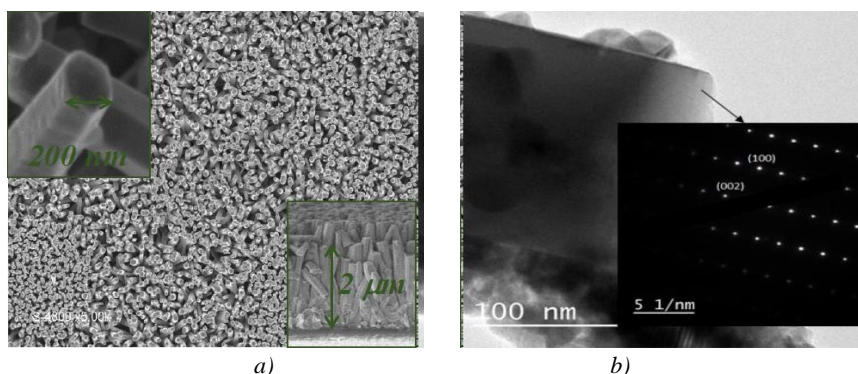


Fig. 2. (a) SEM Images of the ZnO Nanorods, the insets shows the top view of initial ZnO NR arrays; (b) High resolution electron microscopy image of a ZnO rod and its corresponding diffraction along the [010] zone axis showing a high crystalline quality .

The X-ray diffraction analysis was carried out using the INEL powder diffractometer equipped with a curved linear detector that covers a large angular range of 120°. An Si monochromator ensures the focusing of the beam on the detector. The radiation used is from a Cu

anode ($K\alpha$, $\lambda = 0.154$ nm) with a high precision and a real time acquisition. The samples are arranged in vertically positioned capillaries.

Fig. 3 (a) is the XRD patterns of the as-prepared ZnO NR arrays. It can be seen that the XRD pattern matches well with the standard XRD pattern of Cu_2ZnSnS_4 (JCPDS No. 26-0575). All the peaks can be attributed to hexagonal ZnO. Moreover, the strong intensity of the (002) diffraction peak located at about $2\theta = 34.5^\circ$ and three diffraction peaks at $2\theta = 26.5, 47.3,$ and 64.8° are observed, which are indexed to diffraction of the (220), (331), and (331) planes of tetragonal CZTS respectively.

confirms that the product grown on the substrate has a preferential growth direction along the c-axis orientation. No impurities or impurity phases such as SnS, SnS_2 or Cu_xS were detected in the diffraction pattern., indicating that this ZnO sample is highly phase-pure. The diffraction peaks can be indexed to hexagonal CZTS and hexagonal ZnO.

Because some of the diffraction peaks of CZTS and ZnO stand too close to be distinguished, the structure was further investigated by Raman spectrum. The Figure. 3b shows the Raman spectrum of the structure. From the Raman spectrum we can observe one major peak at 333 cm^{-1} as well as two small peaks at 287 cm^{-1} and 270 cm^{-1} . All these peaks are well defined as the characteristic peaks of Cu_2ZnSnS_4 in Raman spectrum [21,22]. So the existence of ZnO in the structure is excluded by the Raman test and all the diffraction peaks in the XRD pattern are attributable to CZTS. From the XRD and Raman test we can conclude that the precursor transforms to CZTS phase during the annealing, and no obvious impurity phases are formed during this process.

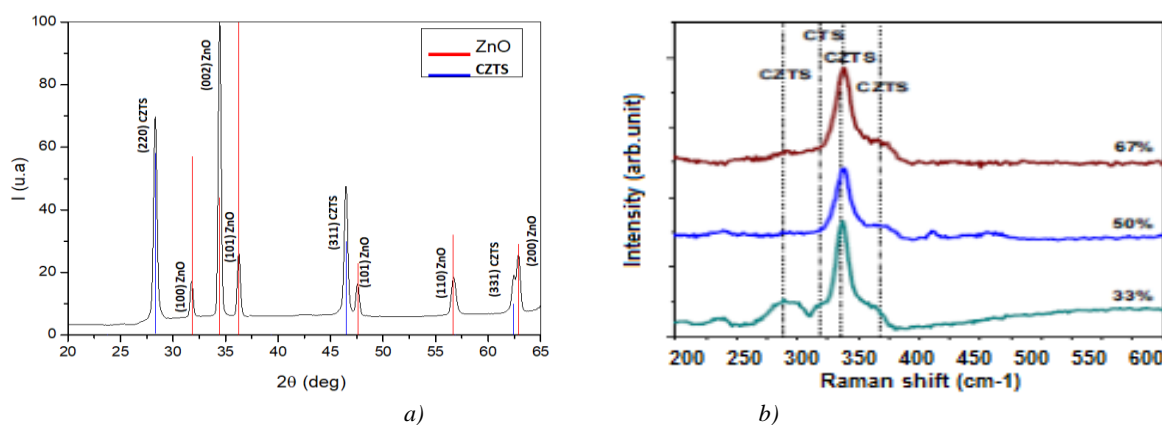


Fig. 3. (a) XRD pattern and (b) Raman spectrum of the CZTS film.

Fig. 4 presents a high resolution transmission electron microscopy image obtained on sample of ZnO/CZTS heterostructure NR arrays. It can be observed that CZTS nanoparticles have grown on the surface of ZnO NR. Moreover, in some areas, the space between NRs have been filled up. The surface of NRs becomes rougher after the penetration of CZTS nanoparticles.

High resolution transmission electron microscopy image of show a twinned domains on the CZTS nanocrystals and its Fourier transform, along [011] zone axis, showing a splitting of the Bragg spot's. The twinned part of the CZTS nanocrystal is associated to the weaker intensity spot.

The magnification of CZTS nanocrystals pattern shows a quite significant contrast variation in the image due to the presence of microtwins. The study of the contrast's image divulge an atomic arrangement of the CZTS / ZnO interface which is done by the intersection of the twinned CZTS with a perfectly monocrystalline atomic arrangement of ZnO. The effect of this reconstruction is reflected in a multiplicity of periodicity along the junction line. This new periodicity is stabilized by local relaxations, which explains the perfect adhesion of CZTS on ZnO.

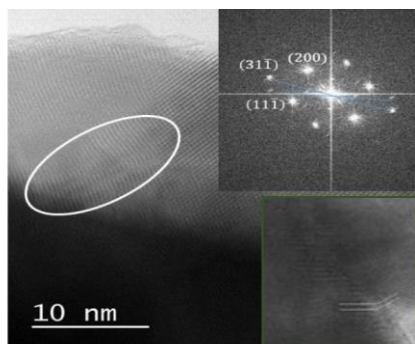


Fig. 4. High resolution transmission electron microscopy image obtained on sample of the CZTS nanocrystal on ZnO. the insets shows the twinned domains on the CZTS nanocrystals and its Fourier transform, along [011] zone axis and the magnification at the interface showing the doubling of the CZTS cell parameter at the junction.

4. Conclusion

In this paper we show a good crystalline quality both of ZnO rods and CZTS nanocrystals. The results of HRTEM reveal a twinning of CZTS nanocrystals similar to that encountered in the bulk materials in its single crystal form. Our analysis showed CZTS film showed the kesterite phase, although minor impurity phases were observed. these research results open the viability of CZTS thin film solar cell in flexible and conformal device platforms.

Acknowledgements

This work was supported by the grant of the University of Tabuk, Saudi Arabia [Grant S-0191-1439].

References

- [1] K. Ito, T. Nakazawa, Jpn. J. Appl. Phys. **27**, 2094 (1988).
- [2] K. Ito, T. Nakazawa, Proc. 4th Int. Conf. Photovoltaic Science and Engineering, p. 341, 1989.
- [3] N. Nakayama, K. Ito, Appl. Surf. Sci. **92**, 171 (1996).
- [4] M. Altosaar, J. Raudoja, K. Timmo, M. Danilson, M. Grossberg, J. Krustok, E. Mellikov, Phys. Status Solidi A **205**, 167 (2008).
- [5] T. K. Todorov, K. B. Reuter, David B. Mitzi, Adv. Mater. **22**, E156 (2010).
- [6] M. A. Green, K. Emery, Y. Hishikawa, W. Warta, Prog. Photovoltaics **17**, 85 (2009).
- [7] D. Butler, Nature **454**, 558 (2008).
- [8] G. Zoppi, I. Forbes, R. W. Miles, P. J. Dale, J. J. Scragg, L. M. Peter, Prog. Photovoltaics **17**, 315 (2009).
- [9] A. Redinger, D. M. Berg, P. J. Dale, S. Siebentritt, Journal of the American Chemical Society **133**(10), 3320 (2011).
- [10] A. Redinger, K. Hones, X. Fontané, V. Izquierdo-Roca, Applied Physics Letters **98**(10), 101907 (2011).
- [11] K. Wang, B. Shin, K. B. Reuter, T. Todorov, Applied Physics Letters **98**(5), 051912 (2011).
- [12] S. Ahn, S. Jung, J. Gwak, A. Cho, Applied Physics Letters **97**(2), 021905 (2010).
- [13] P. Salomé, P. Fernandes, A. da Cunha, Thin Solid Films **517**(7), 2531 (2009).
- [14] O. Volobujeva, J. Raudoja, E. Mellikov, M. Grossberg, Journal of Physics and Chemistry of Solids **70**(3–4), 567(2009)
- [15] H. Katagiri, K. Jimbo, W. S. Maw, K. Oishi, M. Yamazaki, H. Araki, A. Takeuchi, Thin Solid

- Films **517**, 2455 (2009).
- [16] H. Katagiri, K. Jimbo, S. Yamada, T. Kamimura, W. S. Maw, T. Fukano, T. Ito, T. Motohiro, *Appl. Phys. Express* **1**, 041201 (2008).
- [17] H. Katagiri, K. Jimbo, R. Kimura, T. Kamimura, S. Yamada, W. S. Maw, H. Araki, K. Oishi, *Thin Solid Films* **515**, 5997 (2007).
- [18] S. Chen, X. G. Gong, A. Walsh, S. H. Wei, *Appl. Phys. Lett.* **96**, 021902 (2010).
- [19] S. Chen, J. H. Yang, X. G. Gong, A. Walsh, S. H. Wei, *Phys. Rev. B* **81**, 245204 (2010).
- [20] R. Schurr, A. Holzing, S. Jost, R. Hock, T. Vo, B. J. Schulze, A. Kirbs, A. Ennaoui, M. Lux-Steiner, A. Weber, I. Kotschau, H.-W. Schock, *Thin Solid Films* **517**, 2465 (2009).
- [21] A. Ennaoui, M. Lux-Steiner, A. Weber, D. Abou-Ras, I. Kotschau, H. W. Schock, R. Schurr, A. Holzing, S. Jost, R. Hock, T. Vo, B. J. Schulze, A. Kirbs, *Thin Solid Films* **517**, 2511 (2009).
- [22] N. Izyumskaya, V. Avrutin, U. Ozgur, Y. I. Alivov, H. Morkoc, *Phys. Status Solldi B* **244**, 1439 (2007).
- [23] C. Kittel, *Introduction to Solid State Physics*, Wiley, New York, 8th ed., p. 190, 2005.